Chen *et al.*
Natural Products and Bioprospecting (2026) 16:81
https://doi.org/10.1007/s13659-026-00610-6

Natural Products and Bioprospecting

ORIGINAL ARTICLE Open Access

Wuchuyuamines A-G, seven new alkaloids isolated from the fruits of *Tetradium ruticarpum* and their antifungal activities

Meng-Ting Chen[1,3], Jian Zhang[1], Qian Zhao[1,3], Su-Min Zhang[1], Yin-Ling Wei[1,3], Ying Zhang[1] and Xiao-Jiang Hao[1,2,3,4*]

Abstract

Plant diseases caused by fungal pathogens severely threaten crop yields and food security, driving the need for new, environmentally friendly fungicides. In this study, thirty-six alkaloids, including seven novel ones (**1**–**4**, **23**, **29**, and **30**), were isolated from the fruits of *Tetradium ruticarpum*, and their structures were elucidated by extensive spectroscopic analyses. The antifungal potential of compounds obtained with sufficient quantities was evaluated using the mycelial growth rate method against three phytopathogens (*Alternaria solani*, *Bipolaris sorokiniana*, and *Fusarium odoratissimum*). Compounds **16** and **24** showed notable activity against *A. solani*, exhibiting approximately 80% and 90% growth inhibition at 100 μg/mL, with IC_{50} values of 33.39 and 36.02 μg/mL, respectively. To evaluate the antifungal spectrum, the abundant constituents **13**, **19**, and **25** were further screened against sixteen phytopathogenic fungi. Among them, compound **25** displayed the most potent and broad-spectrum antifungal activity, achieving an IC_{50} of 13.15 μg/mL against *Fusarium graminearum*, which was stronger than the positive control hymexazol. Furthermore, SEM and TEM analyses revealed that compound **25** markedly disrupted the surface morphology and cellular ultrastructure, suggesting a potential link to membrane integrity impairment. Additionally, leakage assays showed increased release of nucleic acids and proteins, providing evidence that compound **25** increased membrane permeability and compromised the membrane integrity in *F. graminearum*. Therefore, compound **25** represents a promising lead structure for the development of novel, eco-friendly fungicides.

Keywords *Tetradium ruticarpum*, Alkaloids, Antifungal activity, *Fusarium graminearum*

*Correspondence:
Xiao-Jiang Hao
haoxj@mail.kib.ac.cn
Full list of author information is available at the end of the article

Springer

Graphical Abstract

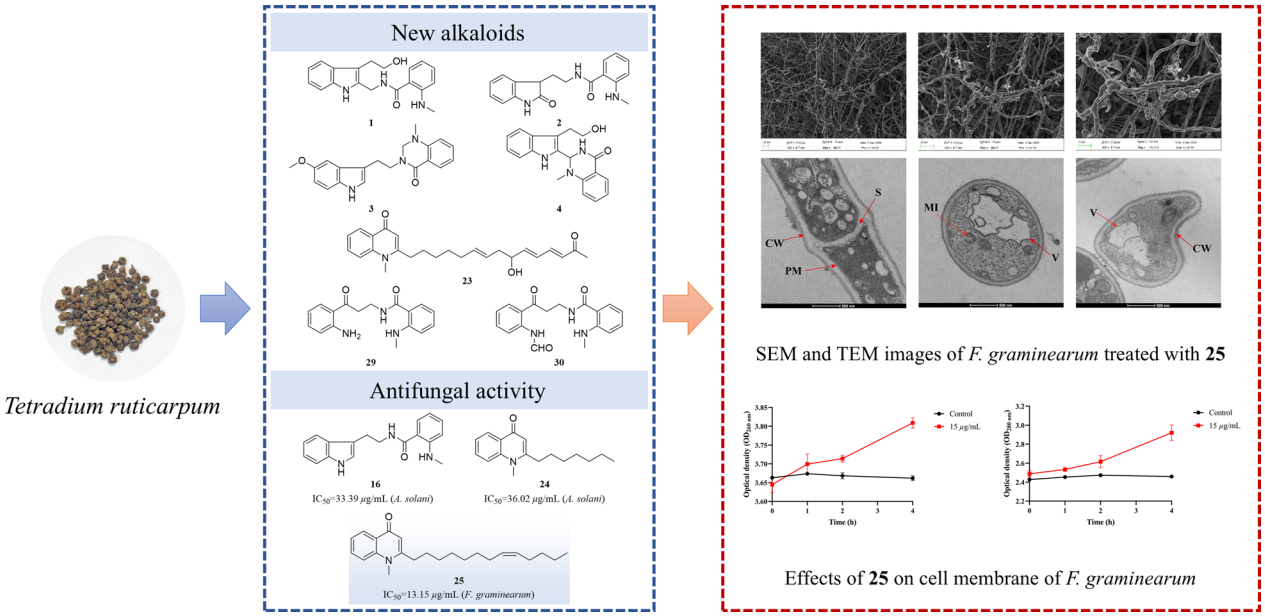

1 Introduction

Plant pathogens cause a wide range of diseases in fruits, vegetables, and other crops, resulting in substantial yield losses and posing a major threat to global agricultural production and food security. Approximately 8000 species of fungi and oomycetes have been reported to be associated with plant diseases [1, 2]. Among fungal pathogens, *Magnaporthe oryzae*, *Botrytis cinerea*, *Puccinia* spp., *Fusarium graminearum*, and *Fusarium oxysporum* are the most scientifically and economically important fungal pathogens [3]. Chemical control remains the most widely used approach for managing plant diseases. However, the excessive and long-term application of synthetic fungicides has led to multiple problems, including environmental pollution, potential health risks to humans and animals, and the emergence of fungicide-resistant pathogens [4]. These issues have prompted an urgent demand for safer and more sustainable alternatives.

To meet this demand, the development of plant-derived natural products as sources of fungicidal agents is consistent with future-oriented food and agricultural policies [5]. Among these natural products, alkaloids, a class of nitrogen-containing heterocyclic compounds, have garnered increasing attention due to their relatively low mammalian toxicity, ready biodegradability, and environmental compatibility [6, 7]. *Tetradium ruticarpum* (A. Juss.) T. G. Hartley (Rutaceae family, *Tetradium* genus), known as Wu Zhu Yu in traditional Chinese medicine, has been widely used for centuries to treat ailments such as headache, abdominal pain, and vomiting [8]. Phytochemical investigations have revealed that *T. ruticarpum* contains diverse bioactive constituents, including alkaloids, limonoids, and flavonoids [9–11]. To date, approximately 300 metabolites have been reported in *T. ruticarpum*, about half of which are alkaloids [12]. Pharmacological studies further indicate that these constituents exhibit diverse biological activities, such as vasodilatory, anti-inflammatory, analgesic, and antibacterial effects [13, 14]. Nevertheless, the antifungal potential of alkaloids derived from *T. ruticarpum* remains largely unexplored.

In this study, we aimed to systematically isolate and identify the alkaloids from the fruits of *T. ruticarpum* and evaluate their antifungal activities against phytopathogenic fungi. A total of thirty-six alkaloids were obtained (Fig. 1), including seven new ones (**1**–**4**, **23**, **29**, and **30**) and twenty-nine known alkaloids: rutaecarpine (**5**) [15], 3-hydroxyrutaecarpine (**6**) [16], evodiamine (**7**) [15], 3-hydroxyevodiamine (**8**) [17], N^{14}-formyldihydrorutaecarpine (**9**) [18], evodamide A (**10**) [19], evollionines A (**11**) [20], goshuyuamide I (**12**) [21], 1,2,3,4-tetrahydronorharman-1-one (**13**) [22], goshuyuamide II (**14**) [21], 3-(2-(1H-indol-3-yl)ethyl)quinazolin-4(3H)-one (**15**) [23], *N*-(2-methylaminobenzoyl)tryptamine (**16**) [24], evodiamide (**17**) [25], wuchuyuamide II (**18**) [26], wuchuyuamide I (**19**) [26], evollionines B (**20**) [20],

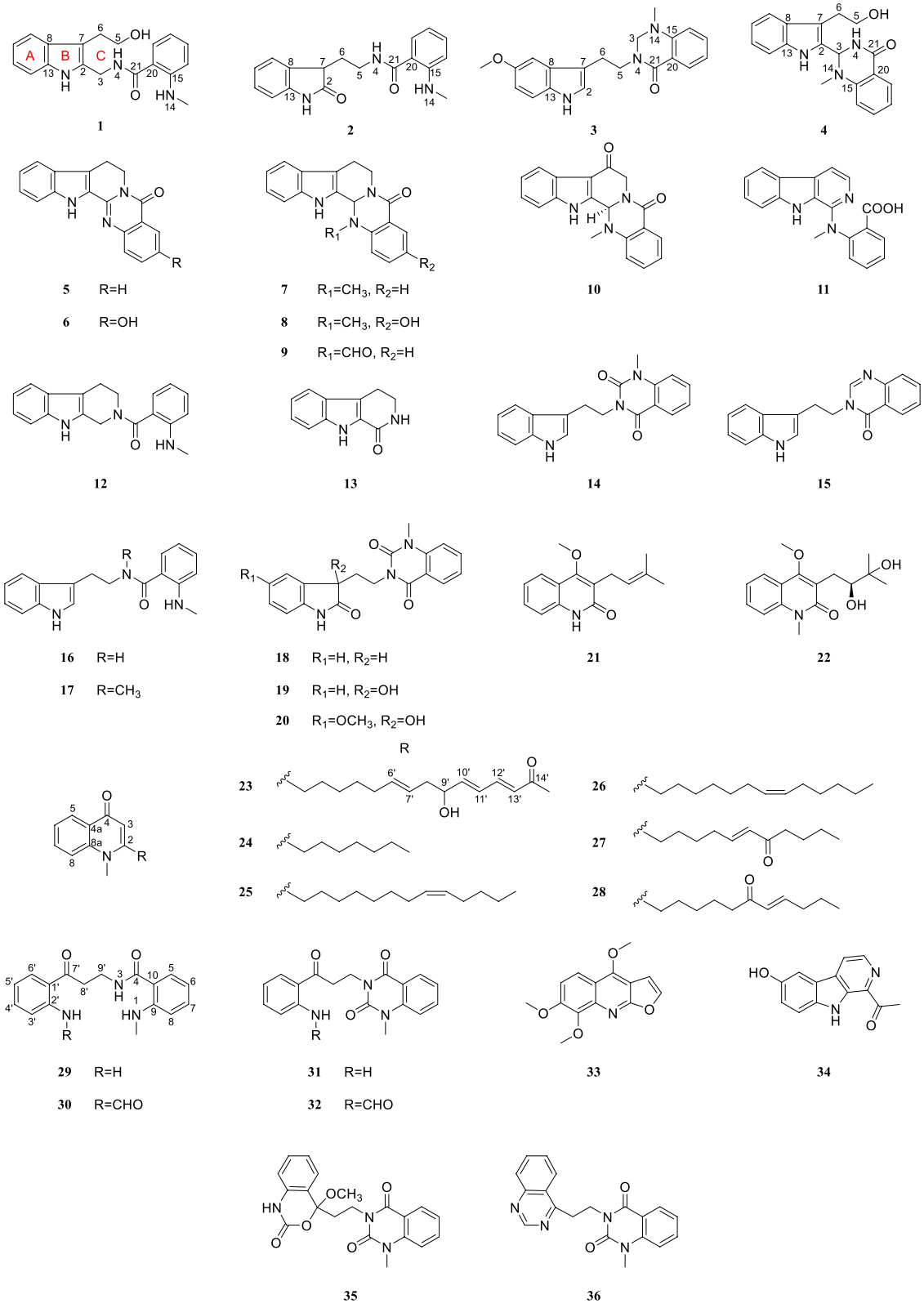

Fig. 1 The structures of compounds **1**–**36**

atanine (**21**) [27], edulinine (**22**) [28], 2-heptyl-1-methyl-4(1*H*)-quinolinone (**24**) [29], evocarpine (**25**) [30], 1-methyl-2-[(*Z*)-7-tridecenyl]-4(1*H*)-quinolinone (**26**) [31], euocarpine A (**27**) [32], euocarpine B (**28**) [32], wuchuyuamide III (**31**) [33], wuchuyuamide IV (**32**) [34], skimmianine (**33**) [35], sinometumine I (**34**) [36], evodiamide A (**35**) [37], and evodiamide B (**36**) [37]. Their structures were elucidated based on extensive spectroscopic analyses. Compounds **8**, **15**, **22**, and **34** were reported from *T. ruticarpum* for the first time. This report described the isolation and structural elucidation of all alkaloids obtained from *T. ruticarpum*, and the antifungal activities of selected compounds were further assessed.

2 Results and discussion

2.1 Structure elucidation and identification

Wuchuyuamine A (**1**) was acquired as a yellow amorphous powder and its molecular formula $C_{19}H_{21}N_3O_2$ was determined by HRESIMS at *m/z* 346.1533 $[M+Na]^+$ (calcd. for $C_{19}H_{21}N_3O_2Na$, 346.1526) with 11 degrees of unsaturation. The ^1H NMR data (CD_3OD, 500 MHz; Table 1) of compound **1** revealed two 1,2-disubstituted aromatic rings [δ_H 7.49 (1H, d, J=7.8 Hz, H-9), δ_H 6.98 (1H, ddd, J=8.0, 7.0, 1.1 Hz, H-10), δ_H 7.06 (1H, ddd, J=8.1, 7.1, 1.2 Hz, H-11), δ_H 7.29 (1H, m, H-12); δ_H 6.68 (1H, d, J=8.4 Hz, H-16), δ_H 7.29 (1H, m, H-17), δ_H 6.56 (1H, dd, J=8.0, 7.0 Hz, H-18), δ_H 7.46 (1H, dd, J=7.9, 1.6 Hz, H-19)], three aliphatic methylene signals [δ_H 4.66 (2H, s, H-3), δ_H 3.78 (2H, t, J=6.8 Hz, H-5), δ_H 3.03 (2H, t, J=6.8 Hz, H-6)], and an *N*-CH_3 signal [δ_H 2.83 (3H, s, *N*-CH_3)]. In addition, the ^{13}C NMR, DEPT, and HSQC data showed seven quaternary carbon signals, including six aromatic carbon signals [δ_C 133.9 (C-2), 110.4 (C-7), 129.4 (C-8), 137.4 (C-13), 151.6 (C-15), 116.9 (C-20)] and an amide carbon signal [δ_C 172.2 (C-21)]. These data indicated that compound **1** was an indolequinazoline alkaloid. The structure could be determined through further 2D NMR analysis. In the ^1H-^1H COSY spectrum, the cross peak of H_2-5/H_2-6 confirmed the presence of a CH_2CH_2 alkyl fragment. The HMBC correlations from H_2-5 to C-7 and from H_2-6 to C-2/C-7/C-8 indicated that C-7 on the indole ring was connected to the CH_2CH_2 alkyl fragment. The HMBC correlations from H_2-3 to C-2/C-7/C-21 demonstrated that the quinazoline unit was connected to the indole ring through C-3 (Fig. 2). Along with the molecular formula of compound **1** and the chemical shift of C-5 (δ_C 63.4) suggested that C-5

Table 1 ^1H NMR and ^{13}C NMR spectroscopic data for **1**–**4** (δ in ppm, J in Hz)

No	1[a]		2[b]		3[c]		4[a]	
	δ_H	δ_C	δ_H	δ_C	δ_H	δ_C	δ_H	δ_C
2		133.9		179.8	7.08 (1H, s)	124.5		132.4
3	4.66 (2H, s)	36.0			4.21 (2H, s)	68.1	5.98 (1H, s)	67.9
5	3.78 (2H, t, 6.8)	63.4	3.58 (2H, m)	37.8	3.80 (2H, t, 7.0)	48.5	3.80 (2H, m)	63.3
6	3.03 (2H, t, 6.8)	28.5	2.18 (2H, m)	31.3	3.08 (2H, t, 7.0)	25.0	3.06 (2H, m)	28.4
7		110.4	3.53 (1H, d, 6.0)	44.8		113.0		113.9
8		129.4		130.7		129.1		128.8
9	7.49 (1H, d, 7.8)	119.2	7.40 (1H, d, 7.4)	125.1	7.09 (1H, d, 2.4)	101.2	7.58 (1H, d, 8.0)	119.8
10	6.98 (1H, ddd, 8.0, 7.0, 1.1)	119.7	7.00 (1H, dd, 7.6, 7.5)	122.5		155.0	7.04 (1H, ddd, 8.0, 6.9, 1.0)	120.1
11	7.06 (1H, ddd, 8.1, 7.1, 1.2)	122.4	7.20 (1H, dd, 7.8, 7.6)	128.6	6.74 (1H, dd, 8.7, 2.4)	112.9	7.14 (1H, ddd, 8.2, 7.0, 1.1)	123.7
12	7.29 (1H, m)	112.0	6.92 (1H, d, 7.7)	110.2	7.22 (1H, d, 8.7)	112.9	7.36 (1H, d, 8.2)	112.6
13		137.4		143.5		133.3		138.1
15		151.6		151.7		151.2		151.0
16	6.68 (1H, d, 8.4)	112.0	6.64 (1H, d, 8.3)	111.4	6.72 (1H, d, 8.4)	113.3	6.91 (1H, m)	114.0
17	7.29 (1H, m)	133.8	7.27 (1H, dd, 8.6, 7.1)	133.2	7.40 (1H, dd, 8.3, 7.2)	134.9	7.48 (1H, dd, 7.3, 1.7)	135.8
18	6.56 (1H, dd, 8.0, 7.0)	115.9	6.52 (1H, dd, 7.9, 7.1)	114.8	6.86 (1H, dd, 7.5, 7.5)	119.6	6.91 (1H, m)	119.5
19	7.46 (1H, dd, 7.9, 1.6)	129.3	7.54 (1H, d, 7.9)	128.6	7.83 (1H, d, 7.7)	129.3	7.88 (1H, dd, 7.9, 1.7)	129.2
20		116.9		116.1		118.6		117.2
21		172.2		170.4		165.6		166.4
N-CH_3	2.83 (3H, s)	29.9	2.82 (3H, s)	30.0	2.63 (3H, s)	35.6	2.65 (3H, s)	34.2
OCH_3					3.72 (3H, s)	56.2		

[a] 500 MHz in CD_3OD; 125 MHz in CD_3OD

[b] 600 MHz in $(CD_3)_2CO$; 150 MHz in $(CD_3)_2CO$

[c] 600 MHz in CD_3OD; 150 MHz in CD_3OD

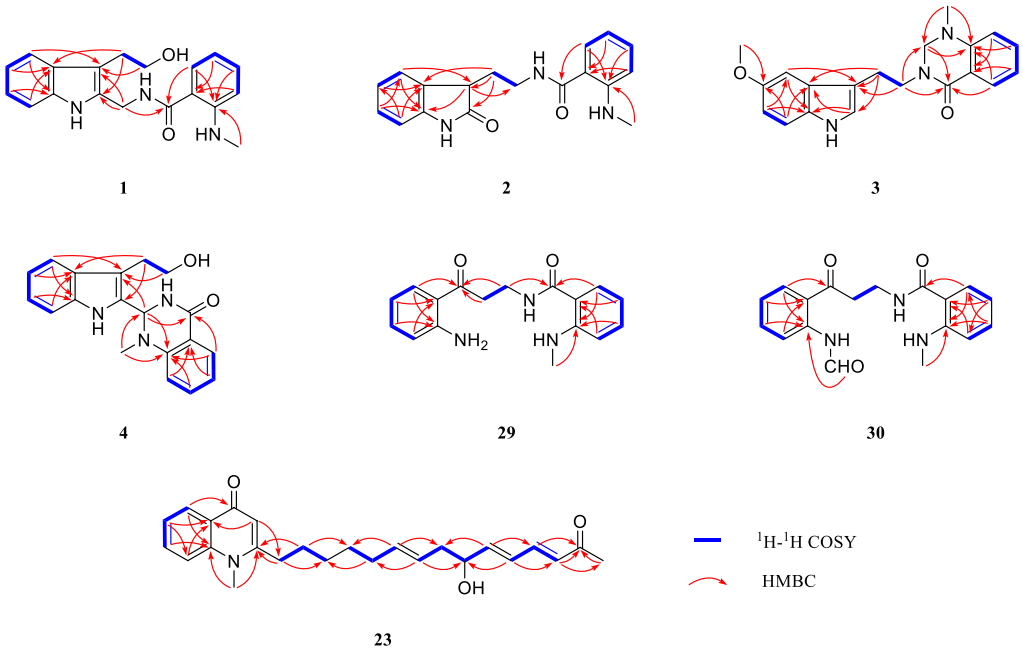

Fig. 2 Key ^{1}H–^{1}H COSY and HMBC correlations of compounds **1**–**4**, **23**, **29**, and **30**

was connected to a hydroxyl group. Comparing with the structure of goshuyuamide I (**12**) [21], the notable difference was that **1** was a C-*seco* indolequinazoline alkaloid with a 5-hydroxyl group. Therefore, the structure of compound **1** was established as depicted in Fig. 1.

Wuchuyuamine B (**2**) was obtained as a white amorphous powder. Its molecular formula was determined as $C_{18}H_{19}N_3O_2$ based on HRESIMS ion peak at *m/z* 310.1547 $[M+H]^+$ (calcd. for $C_{18}H_{20}N_3O_2$, 310.1550). The ^{1}H NMR (CD_3OD, 600 MHz; Figure S12.1) signals of compound **2** were significantly broadened, rendering the spin–spin coupling constants unmeasurable and thereby complicating the structural analysis. Therefore, derivatization of compound **2** was attempted by using chemical approach with hydrogen chloride-methanol solution. After converting **2** into the wuchuyuamine B chloride, the signal broadening disappeared, and coupling constants could be easily measured. The 1D NMR data (^{1}H NMR, 600 MHz; ^{13}C NMR, 150 MHz), recorded in $(CD_3)_2CO$ (see Table 1), indicated that compound **2** had a high degree of structural similarity to *N*-(2-methylaminobenzoyl)tryptamine (**16**) [24]. However, compound **2** had an indolinone unit rather than an indoline unit due to the signals of the indole ring showed significant changes compared with those in *N*-(2-methylaminobenzoyl)tryptamine (**16**), particularly the downfield shift of C-2 (δ_C 179.8, $\Delta\delta$ + 56.3 ppm) and the upfield shift of C-7 (δ_C 44.8, $\Delta\delta$—68.7 ppm). Furthermore, the HMBC correlations from H-7 to C-2/C-5/C-13 were observed, indicating that the double bond placed at C-2 and C-7 in *N*-(2-methylaminobenzoyl)tryptamine (**16**) was replaced by a carbonyl group in compound **2** (Fig. 2). Although compounds *N*-(2-methylaminobenzoyl)tryptamine (**16**) and **2** had similar structures, the ^{1}H NMR spectrum of *N*-(2-methylaminobenzoyl)tryptamine (**16**) did not exhibit broadening signals. The broadening signals of the ^{1}H NMR spectrum of compound **2** were attributed to the existence of an amide moiety, and the 4-NH as an active hydrogen capable could form the intermolecular hydrogen bond with the carbonyl group at C-2. In addition, the specific rotation value of compound **2** was close to zero. Combined with ECD experiments showing no obvious Cotton effect (Figure S17) and the presence of only one chiral center at C-7, compound **2** was determined to be a racemic mixture, and named wuchuyuamine B.

Wuchuyuamine C (**3**) was obtained as a white amorphous powder. Based on the HRESIMS ion peak at *m/z* 358.1529 $[M+Na]^+$ (calcd. for $C_{20}H_{21}N_3O_2Na$, 358.1526), its molecular formula was determined as $C_{20}H_{21}N_3O_2$. Analysis of the ^{1}H and ^{13}C NMR data (600 and 150 MHz, respectively, in CD_3OD; Table 1) for compound **3** revealed a similar structure to 10-methoxygoshuyuamide-II [19]. The molecular weight of compound **3** was 14 less than that of 10-methoxygoshuyuamide-II, and this difference was due to the presence of a carbonyl substitution at C-3 in 10-methoxygoshuyuamide-II. The HMBC correlations from H_2-3 to C-5/C-15/C-21/*N*–CH_3, and from H_2-5 to C-3/C-7/C-21 confirmed the above

speculation (Fig. 2), and therefore the structure of compound **3** was determined as wuchuyuamine C.

Wuchuyuamine D (**4**) was isolated as a white amorphous powder. The molecular formula $C_{19}H_{19}N_3O_2$ was determined by HRESIMS ion peak at *m/z* 322.1554 $[M+H]^+$ (calcd. for $C_{19}H_{20}N_3O_2$, 322.1550). The ^1H NMR (500 MHz, CD_3OD) and ^{13}C NMR (125 MHz, CD_3OD) data (Table 1) displayed signals corresponding to indole and quinazoline rings, indicating that it was an indolequinazoline alkaloid with a similar skeleton to evodiamine (**7**) [15]. Comparison with the ^{13}C NMR data of evodiamine (**7**) suggested that C-5 (δ_C 63.3) and C-6 (δ_C 28.4) in compound **4** were shifted downfield and the chemical shifts were close to C-5 (δ_C 63.4) and C-6 (δ_C 28.5) in compound **1**. The HMBC spectrum of compound **4** also lacked the correlations from H-5 to C-3/C-21 (Fig. 2). Similar to compound **1**, the C ring of compound **4** was broken with the bond disruption of the C-5 and *N*-4, and a hydroxyl group was linked to C-5. The specific rotation was close to zero, and the experimental ECD spectra showed no obvious Cotton effect (Figure S34). Therefore, compound **4** was determined to be a racemic mixture, the structure was depicted as shown in Fig. 1.

Wuchuyuamine E (**23**) was obtained as a yellow oil. Its molecular formula was determined to be $C_{25}H_{31}NO_3$ based on the HRESIMS ion peak at *m/z* 394.2380 $[M+H]^+$ (calcd. for $C_{25}H_{32}NO_3$, 394.2377). The UV spectrum showed absorption maxima at 215, 239, 322, and 335 nm, which were characteristic of the *N*-methyl-4(1*H*)-quinolone skeleton, indicating that compound **23** was a quinolone alkaloid. The ^1H and ^{13}C NMR data (500 and 125 MHz, respectively, in CD_3OD; Table 2) also displayed characteristic signals of the *N*-methyl-4(1*H*)-quinolone skeleton [δ_H 6.31 (1H, s, H-3), 8.32 (1H, dd, J=8.1, 1.5 Hz, H-5), 7.47 (1H, ddd, J=7.9, 6.8, 1.1 Hz, H-6), 7.80 (1H, ddd, J=8.7, 6.8, 1.6 Hz, H-7), 7.86 (1H, dd, J=8.8, 1.3 Hz, H-8), 3.89 (3H, s, *N*-CH_3); δ_C 158.8 (C-2), 111.1 (C-3), 179.5 (C-4), 126.9 (C-4a), 126.6 (C-5), 125.1 (C-6), 133.9 (C-7), 117.9 (C-8), 143.5 (C-8a), 35.5 (*N*-CH_3)]. Combined with the ^1H-^1H COSY and HSQC, the signals of the aliphatic side chain were assigned as [δ_C 35.6, 29.5, 30.2, 29.9, 28.2, 133.1, 126.0, 36.0,72.5, 148.0, 128.9, 145.3, 131.1, 201.4, 27.1 (C1′-C15′)]. In the ^1H-^1H COSY spectrum, the correlations of H-7′/H-8′/H-9′/H-10′, combined with HMBC correlations from H-10′ to C-8′/C-12′, from H-11′ to C-9′/C-13′ (Fig. 2), along with their chemical shifts, indicated the hydroxyl group located at the position of C-9′. Additionally, HMBC correlations from H-3 to C-1′ and from H-2′ to C-2 confirmed that the aliphatic carbon chain was connected to C-2. Based on the coupling constants ($^3J_{H\text{-}6',H\text{-}7'}$=18.1 Hz, $^3J_{H\text{-}10',H\text{-}11'}$=15.3 Hz, $^3J_{H\text{-}12',H\text{-}13'}$=15.6 Hz), the configurations of the couple of olefinic carbons between C-6′ and C-7′, between C-10′ and C-11′, between C-12′ and C-13′ in compound **23** were elucidated as *E*-form. Compound **23** was further confirmed to be a racemate because it showed no Cotton effect and its optical rotation value was close to zero (Figure S43). From above mentioned results, the structure of **23** was elucidated as wuchuyuamine E.

Table 2 ^1H NMR (500 MHz) and ^{13}C NMR (125 MHz) spectroscopic data for **23** in CD_3OD (δ in ppm, J in Hz)

No	δ_H	δ_C	No	δ_H	δ_C
N-CH_3	3.89 (3H, s)	35.5	4′	1.48 (2H, m)	29.9
2		158.8	5′	2.10 (2H, m)	28.2
3	6.31 (1H, s)	111.1	6′	5.51 (1H, dt, 18.2, 7.3)	133.1
4		179.5	7′	5.43 (1H, dt, 18.1, 7.2)	126.0
4a		126.9	8′	2.32 (2H, m)	36.0
5	8.32 (1H, dd, 8.1, 1.5)	126.6	9′	4.21 (1H, dt, 6.6, 5.3)	72.5
6	7.47 (1H, ddd, 7.9, 6.8, 1.1)	125.1	10′	6.27 (1H, dd, 15.3, 5.7)	148.0
7	7.80 (1H, ddd, 8.7, 6.8, 1.6)	133.9	11′	6.41 (1H, dd, 15.4, 11.0)	128.9
8	7.86 (1H, dd, 8.8, 1.3)	117.9	12′	7.25 (1H, dd, 15.7, 10.8)	145.3
8a		143.5	13′	6.14 (1H, d, 15.6)	131.1
1′	2.89 (2H, t, 7.8)	35.6	14′		201.4
2′	1.73 (2H, m)	29.5	15′	2.25 (3H, s)	27.1
3′	1.48 (2H, m)	30.2			

Wuchuyuamine F (**29**) was a white amorphous powder. The HRESIMS ion peak at *m/z* 320.1362 $[M+Na]^+$ (calcd. for $C_{17}H_{19}N_3O_2Na$, 320.1369) and 1D NMR data (^1H NMR, 600 MHz; ^{13}C NMR, 150 MHz), recorded in CD_3OD (Table 3), led to the determination of the molecular formula as $C_{17}H_{19}N_3O_2$. ^{13}C NMR data of **29** indicated a similar structure to wuchuyuamide III (**31**), except for the absence of a carbonyl signal. In the HMBC spectrum (Fig. 2), compound **29** lacked the key correlations from H-9′ to C-2 and from *N*–CH_3 to C-2. Therefore, the absent carbonyl group was located at the position of C-2 and the structure of compound **29** was constructed (Fig. 1).

Wuchuyuamine G (**30**) was obtained as a white amorphous powder. Its molecular formula, $C_{18}H_{19}N_3O_3$, was deduced from the HRESIMS ion peak at *m/z* 326.1499 $[M+H]^+$ (calcd. for $C_{18}H_{20}N_3O_3$, 326.1499). Since **30** exhibited similar UV, IR, and NMR spectral characteristics to **29**, it was supposed that compound **30** had the same skeleton as **29**. Analysis of the ^1H and ^{13}C NMR spectra of **30**, recorded in $CDCl_3$ at 600 and 150 MHz (Table 3), showed an additional aldehyde signal (δ_H 8.52; δ_C 160.0) compared with **29**. Combined with the HMBC correlation from aldehyde proton (δ_H 8.52) to C-2′

Table 3 ^{1}H NMR and ^{13}C NMR spectroscopic data for **29** and **30** (δ in ppm, *J* in Hz)

No	29[a]		30[b]	
	δ_H	δ_C	δ_H	δ_C
4		172.3		170.0
5	7.39 (1H, dd, 7.8, 1.6)	129.1	7.30 (1H, m)	127.3
6	6.58 (1H, m)	115.9	6.58 (1H, dd, 7.6, 7.6)	114.6
7	7.29 (1H, ddd, 8.6, 7.1, 1.6)	133.6	7.30 (1H, m)	133.2
8	6.68 (1H, d, 8.4)	111.9	6.66 (1H, d, 8.3)	111.3
9		151.4		150.8
10		117.4		114.8
N-CH_3	2.83 (3H, s)	29.9	2.85 (3H, d, 5.0)	29.8
1′		118.6		121.6
2′		152.7		140.1
3′	6.74 (1H, d, 8.4)	118.3	8.76 (1H, d, 8.5)	121.9
4′	7.23 (1H, ddd, 8.5, 6.9, 1.5)	135.5	7.58 (1H, dd, 8.0, 7.9)	135.7
5′	6.58 (1H, m)	116.2	7.17 (1H, dd, 7.8, 7.7)	123.4
6′	7.80 (1H, dd, 8.3, 1.5)	132.4	7.94 (1H, d, 8.0)	131.1
7′		202.5		204.0
8′	3.27 (2H, t, 6.8)	39.5	3.39 (2H, t, 5.7)	39.8
9′	3.69 (2H, t, 6.8)	36.8	3.82 (2H, dt, 5.9, 5.8)	34.7
CHO			8.52 (1H, s)	160.0
*N*H-CHO			11.5 (1H, s)	

[a] 600 MHz in CD_3OD; 150 MHz in CD_3OD

[b] 600 MHz in $CDCl_3$; 150 MHz in $CDCl_3$

(Fig. 2), it could be concluded that the aldehyde group and C-2′ were connected through the amino group. The structure of compound **30** was determined as depicted in Fig. 1.

2.2 Antifungal activity in vitro

The antifungal activities of compounds **2**, **4**, **12**–**14**, **16**, **18**, **19**, **24**–**26**, **31,** and **33**, available in sufficient amounts, were evaluated against three phytopathogenic fungi. The results are summarized in Table S1. Among the tested compounds, **16** and **24** exhibited pronounced inhibitory activity against *Alternaria solani*, with inhibition rates approaching 80% and 90% at 100 μg/mL, respectively. To further assess their antifungal potency, the IC_{50} values of **16** and **24** against *A. solani* were determined (Table 4). Both compounds **16** and **24** demonstrated dose-dependent inhibition, although their activities were slightly lower than that of the commercial fungicide hymexazol. These results suggest that the structural frameworks of **16** and **24** may confer selective antifungal activity toward *A. solani.*

To further investigate the broad-spectrum antifungal potential of the major alkaloids in *T. ruticarpum*, compounds **13**, **19** and **25**, identified as the high-content constituents in the fruit extract, were selected for testing

Table 4 Antifungal activities with IC_{50} of compounds **13**, **16**, **24**, **25**

Test fungi	Compounds	IC_{50} (μg/mL)	95% CI	R^2
A. solani	**16**	33.39	29.58–38.26	0.9964
	24	36.02	32.26–40.79	0.9977
	Hymexazol[a]	14.90	11.23–19.92	0.9872
F. graminearum	**13**	> 100	–	–
	25	13.15	8.51–21.36	0.9710
	Hymexazol[a]	30.86	23.61–43.67	0.9829

[a] Hymexazol was used as the positive control

against sixteen phytopathogenic fungi, including *Botrytis* sp., *Ceratocystis fimbriata*, *Colletotrichum capsici f. nicotianae*, *Colletotrichum* sp., *Curvularia lunata*, *Exserohilum turcicum*, *Fusarium graminearum*, *Fusarium moniliforme*, *Fusarium oxysporum*, *Gerlachia nivalis*, *Neofusicoccum* sp., *Pestalotiopsis maculans*, *Pestalotiopsis* sp., *Phytophthora capsici*, *Rhizoctonia solani*, *Verticillium dahliae*, with hymexazol serving as the positive control (Table S2). Among the three alkaloids, compound **25** presented the most pronounced antifungal activity, with inhibition rates varying between 7.2% and 83.5%. Notably, compound **25** showed stronger inhibitory activity against *F. graminearum* than hymexazol, with an IC_{50} value of 13.15 μg/mL (Table 4), highlighting its potential as a promising lead compound for the development of plant-derived fungicides. Additionally, compound **13** showed moderate inhibition activity, with a maximum inhibition rate of 72.9% at 100 μg/mL, depending on the pathogen tested. Unfortunately, compound **19** exhibited negligible inhibitory activity across all tested fungi, indicating limited antifungal potential.

2.3 Observation of morphology and ultrastructure in *F. graminearum*

Scanning Electron Microscopy (SEM) was employed to observe the morphological effects of **25** on *F. graminearum* hyphae, in which the mycelia of *F. graminearum* treated by DMSO were used as blank controls. As shown in Fig. 3A, the hyphae on the PSA medium containing DMSO were slender, uniform, and smooth. In contrast, **25** (15 μg/mL) caused disordered growth and distortion, with a roughened surface, localized collapse and hyphal breakage. These results indicated that **25** caused severe damage to the hyphae of *F. graminearum*.

Transmission Electron Microscopy (TEM) observations further confirmed ultrastructural disruption (Fig. 3B). Control hyphae displayed intact cell walls with well-defined plasma membranes, preserved mitochondria, and normal vacuoles. After treatment with **25** (15 μg/mL), the cell wall contour became deformed

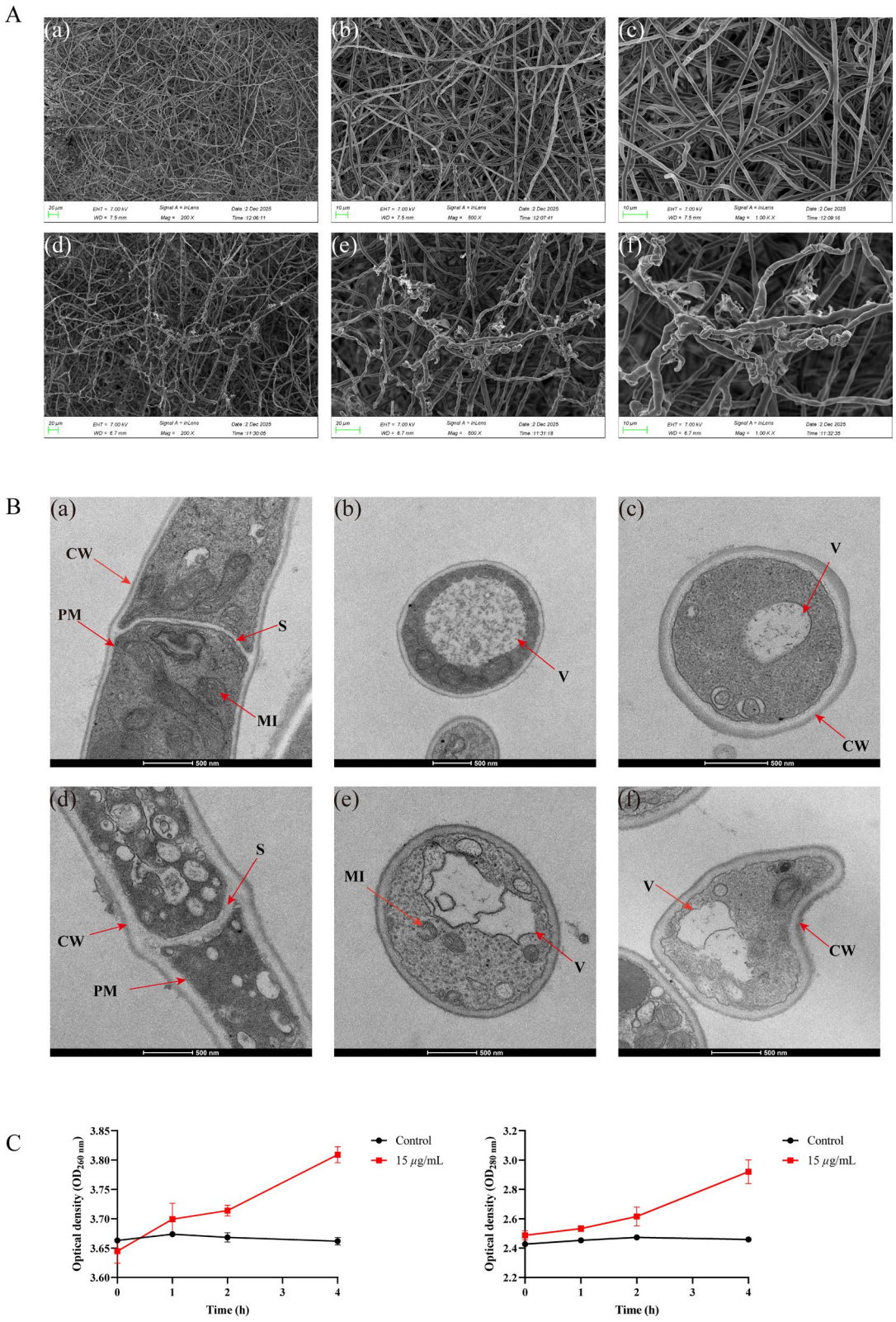

Fig. 3 **A** SEM images [200 × (a, d), 500 × (b, e) and 1000 × (c, f) magnification] of *F. graminearum* hyphae treated with DMSO (a-c) and **25** at 15 μg/mL (d-f). **B** TEM images [22,000 × (a, d-f), 17,500 × (b) and 28,000 × (c) magnification] of *F. graminearum* hyphae treated with DMSO (a-c) and **25** at 15 μg/mL (d-f). Scale bars are provided in each image in (**A**) and (**B**). CW, cell wall; PM, plasma membrane; S, septum; V, vacuole; MI, mitochondrion. **C** Leakage of nucleic acids ($OD_{260\ nm}$) and proteins ($OD_{280\ nm}$)

and the plasma membrane was indistinct, accompanied by pronounced cytoplasmic vacuolization and markedly wrinkled vacuolar membranes. In addition, some mitochondria showed disorganization and compromised membrane integrity. These observations suggest that **25** disrupted the cellular ultrastructure of *F. graminearum.*

2.4 Effect of 25 on the cytoplasmic content leakage of *F. graminearum*

Membrane damage was evaluated by measuring leakage of intracellular components. To assess the effect of **25**, nucleic acid ($OD_{260\ nm}$) and protein ($OD_{280\ nm}$) leakage were quantified. As shown in Fig. 3C, $OD_{260\ nm}$ and $OD_{280\ nm}$ values in the DMSO control remained relatively stable over time. In contrast, treatment with **25** (15 μg/mL) led to a time-dependent increase in $OD_{260\ nm}$ and $OD_{280\ nm}$ within 4 h. This demonstrates that **25** enhanced cell membrane permeability, resulting in membrane rupture and subsequent leakage of intracellular contents.

3 Conclusion

In summary, thirty-six alkaloids, including seven novel compounds, wuchuyuamines A-G (**1**–**4**, **23**, **29**, and **30**), were isolated and identified from the fruits of *T. ruticarpum*. The antifungal activities of representative alkaloids were systematically evaluated against a range of phytopathogenic fungi. Compounds **16** and **24** exhibited moderate inhibitory activity against *A. solani*, with IC_{50} values of 33.39 and 36.02 μg/mL, respectively. Notably, compound **25** demonstrated marked broad-spectrum antifungal efficacy, particularly against *F. graminearum*, where its inhibitory potency (IC_{50} = 13.15 μg/mL) exceeded that of the commercial fungicide hymexazol. The SEM and TEM analyses indicated that **25** disrupted the surface morphology and cellular ultrastructure of *F. graminearum* hyphae. Compound **25** induced leakage of intracellular contents, resulting in metabolic dysregulation and ultimately leading to cell death. These findings not only expand the chemical diversity of alkaloids from *T. ruticarpum* but also highlight the antifungal potential of quinolone alkaloids as promising lead structures for the development of novel, efficient, and environmentally friendly fungicides.

4 Experimental

4.1 General experimental procedures

HRESIMS data were acquired on an Agilent 1260 UPLC/6540 Q-TOF MS spectrometer (Agilent, USA). Optical rotations were measured in MeOH using an Autopol VI spectropolarimeter (Rudolph Research Analytical). ECD spectra were recorded on a Chirascan instrument (Applied Photophysics Ltd., Leatherhead, UK). 1D and 2D NMR spectra were obtained on Bruker 500 or 600 MHz spectrometer with chemical shifts (δ) given in ppm with reference to the solvent and coupling constants (J) in Hz (Bruker, Germany). UV spectra were obtained on a Shimadzu UV-2401PC spectrophotometer (Shimadzu, Tokyo, Japan). IR spectra were recorded on a Bruker Vertex 70 IR spectrometer (Bruker, Germany). Column chromatography was performed using Sephadex LH-20, RP-18, and silica gel. An X-Bridge C_{18} column (Waters, 10 mm × 250 mm, 5 μm) and a YMC-Triart C_{18} column (YMC, 10 mm × 250 mm, 5 μm) were used for HPLC analysis.

4.2 Plant material

The fruits of *T. ruticarpum* were purchased from Chongqing Zhongmiao Pharmaceutical Co., Ltd. (Chongqing, China) in September 2023 (Batch No. 230201). The plant material was identified by Dr. Chun-Lei Xiang, Kunming Institute of Botany, Chinese Academy of Sciences. A voucher specimen (NO. KIBH20230915) was deposited at the State Key Laboratory of Phytochemistry and Natural Medicines, Kunming Institute of Botany, Chinese Academy of Sciences.

4.3 Fungal materials

Plant pathogenic fungi *A. solani*, *Bipolaris sorokiniana* and *Fusarium odoratissimum* were obtained from the Institute of Microbiology, Chinese Academy of Sciences. The remaining fungal strains were supplied by the State Key Laboratory for Conservation and Utilization of Bio-Resources in Yunnan, China.

4.4 Extraction and isolation

The separation and isolation procedures for compounds **1**–**36** and spectroscopic data of **1**–**4**, **23**, **29**, and **30** are provided in the Supporting Information (SI).

4.5 Spectroscopic data

(**1**): yellow amorphous powder; UV (MeOH) λ_{max} (log ε) 207 (4.07), 219 (4.13), 257 (3.58), 278 (3.35), 343 (3.20) nm; IR (KBr) ν_{max} 3433, 1632, 1520, 1384, 1275, 747 cm^{-1}; ^{1}H and ^{13}C NMR data (CD_3OD, 500 and 125 MHz), see Table 1; HRESIMS *m/z* 346.1533 $[M+Na]^+$ (calcd. for $C_{19}H_{21}N_3O_2Na$, 346.1526).

(**2**): white amorphous powder; UV (MeOH) λ_{max} (log ε) 204 (4.53), 241 (4.05), 307 (3.48) nm; IR (KBr) ν_{max} 3390, 2920, 1617, 1582, 1412, 1062, 750 cm^{-1}; ^{1}H and ^{13}C NMR data ($(CD_3)_2CO$, 600 and 150 MHz), see Table 1; HRESIMS *m/z* 310.1547 $[M+H]^+$ (calcd. for $C_{18}H_{20}N_3O_2$, 310.1550).

(**3**): white amorphous powder; UV (MeOH) λ_{max} (log ε) 207 (4.08), 221 (4.15), 297 (3.20), 340 (2.97), 349 (2.94) nm; IR (KBr) ν_{max} 3434, 2924, 1638, 1384, 1215, 759 cm^{-1}; ^{1}H and ^{13}C NMR data (CD_3OD, 600 and 150 MHz), see

Table 1; HRESIMS *m/z* 358.1529 $[M+Na]^+$ (calcd. for $C_{20}H_{21}N_3O_2Na$, 358.1526).

(**4**): white amorphous powder; UV (MeOH) λ_{max} (log ε) 227 (4.83), 268 (4.15), 347 (3.48) nm; IR (KBr) ν_{max} 3390, 3281, 1657, 1488, 1041, 749 cm^{-1}; ^1H and ^{13}C NMR data (CD_3OD, 500 and 125 MHz), see Table 1; HRESIMS *m/z* 322.1554 $[M+H]^+$ (calcd. for $C_{19}H_{20}N_3O_2$, 322.1550).

(**23**): yellow oil; UV (MeOH) λ_{max} (log ε) 215 (3.27), 239 (3.28), 274 (2.88), 322 (2.91), 335 (2.91) nm; IR (KBr) ν_{max} 3433, 2922, 1620, 1598, 1557, 1384, 1268, 1179, 763 cm^{-1}; ^1H and ^{13}C NMR data (CD_3OD, 500 and 125 MHz), see Table 2; HRESIMS *m/z* 394.2380 $[M+H]^+$ (calcd. for $C_{25}H_{32}NO_3$, 394.2377).

(**29**): white amorphous powder; UV (MeOH) λ_{max} (log ε) 208 (3.82), 219 (3.85), 257 (3.45), 355 (3.20) nm; IR (KBr) ν_{max} 3448, 2920, 1637, 1520, 1277, 1210, 1166, 750 cm^{-1}; ^1H and ^{13}C NMR data (CD_3OD, 600 and 150 MHz), see Table 3; HRESIMS *m/z* 320.1362 $[M+Na]^+$ (calcd. for $C_{17}H_{19}N_3O_2Na$, 320.1369).

(**30**): white amorphous powder; UV (MeOH) λ_{max} (log ε) 207 (4.07), 219 (4.14), 225 (4.14), 257 (3.87), 329 (3.48) nm; IR (KBr) ν_{max} 3405, 2922, 1641, 1520, 1277, 1200, 1172, 752 cm^{-1}; ^1H and ^{13}C NMR data ($CDCl_3$, 600 and 150 MHz), see Table 3; HRESIMS *m/z* 326.1499 $[M+H]^+$ (calcd. for $C_{18}H_{20}N_3O_3$, 326.1499).

4.6 Antifungal activity assay in vitro

Compounds **2**, **4**, **12–14**, **16**, **18**, **19**, **24–26**, **31** and **33** were evaluated for their antifungal activities against *A. solani*, *B. sorokiniana* and *F. odoratissimum* at 100 μg/mL following the mycelium growth rate method [38]. For compounds exhibiting appreciable inhibition, dose–response assays were conducted at serial concentrations, and IC_{50} values were calculated from the fitted inhibition curves using the same method. Hymexazol was used as a positive control. All results were expressed as the mean ± SD. Broad-spectrum antifungal activities of compounds **13**, **19** and **25** were further evaluated against sixteen phytopathogenic fungi using the same mycelium growth rate method.

4.7 SEM and TEM observations

Fusarium graminearum was treated with compound **25** at a concentration of 15 μg/mL, while the solvent served as the control. Subsequently, SEM and TEM were used to observe alterations in mycelial morphology and intracellular ultrastructure, respectively [39].

4.8 Effect of 25 on the cytoplasmic content leakage of *F. graminearum*

The mycelium (400 mg) was suspended in 40 mL of sterile water containing **25** (15 μg/mL) and incubated at 26 ℃ for 0, 1, 2, or 4 h, with DMSO as the solvent control. After incubation, the supernatant absorbance at 260 and 280 nm was measured using a SpectraMax iD3 microplate reader (Molecular Devices, USA) to assess nucleic acid and protein leakage, respectively [40].

4.9 Statistical analysis

All experiments were conducted with three independent biological replicates, with consistent results among replicates. The half-maximal inhibitory concentration (IC_{50}) values were calculated by nonlinear regression (log[inhibitor] vs. normalized response, Variable slope) using GraphPad Prism (GraphPad Software, USA). Absorbance at 260 and 280 nm ($OD_{260\,nm}$ and $OD_{280\,nm}$) was analyzed and plotted in GraphPad Prism.

Supplementary Information

The online version contains supplementary material available at https://doi.org/10.1007/s13659-026-00610-6.

Supplementary Material 1. Extraction and isolation; Antifungal activities; 1D and 2D NMR, HRESIMS of compounds **1**–**4**, **23**, **29**, and **30**.

Acknowledgements

We thank the Platform for Plant Multi-dimensional Imaging and Diversity Analysis, Kunming Institute of Botany, Chinese Academy of Sciences, for assistance with SEM and TEM observations.

Author contributions

Meng-Ting Chen: writing—original draft, investigation, formal analysis, data curation. Jian Zhang: formal analysis, data curation. Qian Zhao: formal analysis, data curation. Su-Min Zhang: investigation, data curation. Yin-Ling Wei: investigation. Ying Zhang: data curation. Xiao-Jiang Hao: writing—review and editing, supervision, project administration, funding acquisition, conceptualization. All authors read and approved the final manuscript.

Funding

The present study was supported by the grants from the National Natural Science Foundation of China (82293683), CAMS Innovation Fund for Medical Sciences (CIFMS, 2021-I2M-5-004), Key Research and Development Project of Yunnan Province (202203AC100009), the Project of Yunnan Characteristic Plant Screening and R&D Service CXO Platform (2022YKZY001), and the Open Research Fund of Yunnan Characteristic Plant Extraction Laboratory (YKKF2024005).

Data availability

The data underlying this study are available in the published article and its Supporting Information.

Declarations

Competing interests

The authors declare that there is no competing financial interest in this paper.

Author details

[1]State Key Laboratory of Phytochemistry and Natural Medicines, Kunming Institute of Botany, Chinese Academy of Sciences, Kunming 650201, China. [2]Yunnan Characteristic Plant Extraction Laboratory, Kunming 650106, China. [3]University of Chinese Academy of Sciences, Beijing 100049, China. [4]Research Unit of Chemical Biology of Natural Anti-Virus Products, Chinese Academy of Medical Sciences, Beijing 100730, China.

Received: 3 January 2026 Accepted: 23 February 2026
Published online: 10 August 2026

References

1. Fisher MC, Gurr SJ, Cuomo CA, Blehert DS, Jin H, Stukenbrock EH, et al. Threats posed by the fungal kingdom to humans, wildlife, and agriculture. MBio. 2020;11(3):e00449-e520.
2. Gai YP, Wang HK. Plant disease: a growing threat to global food security. Agronomy. 2024;14(8):1615.
3. Dean R, Van Kan JAL, Pretorius ZA, Hammond-Kosack KE, Di Pietro A, Spanu PD, et al. The top 10 fungal pathogens in molecular plant pathology. Mol Plant Pathol. 2012;13(4):414–30.
4. Ab Rahman SFS, Singh E, Pieterse CMJ, Schenk PM. Emerging microbial biocontrol strategies for plant pathogens. Plant Sci. 2018;267:102–11.
5. Cenobio-Galindo AD, Hernández-Fuentes AD, González-Lemus U, Zaldívar-Ortega AK, González-Montiel L, Madariaga-Navarrete A, et al. Biofungicides based on plant extracts: on the road to organic farming. Int J Mol Sci. 2024;25(13):6879.
6. Dozio D, Sacchi F, Pinto A, Dallavalle S, Annunziata F, Princiotto S. Natural antifungal alkaloids for crop protection: an overview of the latest synthetic approaches. Pharmaceuticals. 2025;18(4):589.
7. Wu YX, Ren D, Gao C, Li JY, Du B, Wang Z, et al. Recent advances for alkaloids as botanical pesticides for use in organic agriculture. Int J Pest Manag. 2021;69(3):288–98.
8. Chinese Pharmacopoeia Commission. Pharmacopoeia of the People's Republic of China. Beijing: China Medical Science and Technology Press; 2025.
9. Li M, Wang C. Traditional uses, phytochemistry, pharmacology, pharmacokinetics and toxicology of the fruit of *Tetradium ruticarpum*: a review. J Ethnopharmacol. 2020;263:113231.
10. Xu XX, Chen JJ, Liang WH, Xu SY, Zhao WL, Wang QZ. Review on chemical constituents and pharmacological activities of genus *Euodia*. Med Plant Biol. 2025;4(1):e019.
11. Zhao ZF, He XR, Han W, Chen XF, Liu PL, Zhao X, et al. Genus *Tetradium* L.: a comprehensive review on traditional uses, phytochemistry, and pharmacological activities. J Ethnopharmacol. 2019;231:337–54.
12. Hao Y, Qi J, Huang X, Liu C, Liu Y. *Euodiae* fructus: a review of botany, application, processing, phytochemistry, quality control, pharmacology, and toxicology. Front Pharmacol. 2025;16:1509032.
13. Choi YH, Shin EM, Kim YS, Cai XF, Lee JJ, Kim HP. Anti-inflammatory principles from the fruits of *Evodia rutaecarpa* and their cellular action mechanisms. Arch Pharm Res. 2006;29(4):293–7.
14. Shan QY, Sang XN, Hui H, Shou QY, Fu HY, Hao M, et al. Processing and polyherbal formulation of *Tetradium ruticarpum* (A. Juss.) Hartley: phytochemistry, pharmacokinetics, and toxicity. Front Pharmacol. 2020;11:133.
15. Zhang H, Yang XW, Chui YX. Complete assignment of ^{1}H and ^{13}C NMR chemical shifts of evodiamine, rutaecarpine and dehydroevodiamine. Chin J Magn Reson. 1999;16(6):563–8.
16. Li XC, Dunbar DC, ElSohly HN, Walker LA, Clark AM. Indolopyridoquinazoline alkaloid from *Leptothyrsa sprucei*. Phytochemistry. 2001;58(4):627–9.
17. Huang G, Kling B, Darras FH, Hellmann J, Decker M. Identification of a neuroprotective and selective butyrylcholinesterase inhibitor derived from the natural alkaloid evodiamine. Eur J Med Chem. 2014;81:15–21.
18. Wang ZJ, Chen YC, Zou FC, Qin Y, Zhu YY, Xiao X, et al. Phytochemical analysis and anti-*Ascaris suum* activity of different *Zanthoxylum* species in vitro and in vivo. J Agric Food Chem. 2023;71(13):5219–29.
19. Li DW, Zhang M, Feng L, Huang SS, Zhang BJ, Liu SS, et al. Alkaloids from the nearly ripe fruits of *Evodia rutaecarpa* and their bioactivities. Fitoterapia. 2020;146:104668.
20. Li YH, He J, Li Y, Wu XD, Peng LY, Du RN, et al. Evollionines A-C, three new alkaloids isolated from the fruits of *Evodia rutaecarpa*. Helv Chim Acta. 2014;97(11):1481–6.
21. Shoji N, Umeyama A, Iuchi A, Saito N, Arihara S, Nomoto K, et al. Two Novel alkaloids from *Evodia rutaecarpa*. J Nat Prod. 1989;52(5):1160–2.
22. Rao KV, Santarsiero BD, Mesecar AD, Schinazi RF, Tekwani BL, Hamann MT. New manzamine alkaloids with activity against infectious and tropical parasitic diseases from an Indonesian sponge. J Nat Prod. 2003;66(6):823–8.
23. Govindan K, Duraisamy T, Jayaram A, Senadi GC, Lin WY. Copper-catalyzed oxidative cyclization of 2-aminobenzamide derivatives: efficient syntheses of quinazolinones and indazolones. Synthesis. 2021;54(4):1115–24.
24. Shoji N, Umeyama A, Iuchi A, Saito N, Takemoto T, Nomoto K, et al. Isolation of an amide, a possible key precursor to evodiamine, from *Evodia rutaecarpa*. J Nat Prod. 1988;51(1):161–2.
25. Shoji N, Umeyama A, Iuchi A, Saito N, Takemoto T, Nomoto K, et al. Isolation of a new alkaloid from *Evodia rutaecarpa*. J Nat Prod. 1988;51(4):791–2.
26. Zuo GY, Yang XS, Hao XJ. Two new indole alkaloids from *Evodia rutaecarpa*. Chin Chem Lett. 2000;11(2):127–8.
27. Reisch J, Müller M, Mester I. Constituents from the rootbark and heartwood of *Afraegle paniculata* (Rutaceae). Planta Med. 1981;43(11):285–9.
28. Wang X, Wanasinghe DN, Zhang J, Ma J, Zhou P, Zhang L, et al. Insights from the endophytic fungi in *Amphisphaeria* (Sordariomycetes): A.*orixae* sp. nov. from *Orixa japonica* and its secondary metabolites. Microorganisms. 2023;11(5):1268.
29. Liu ZL, Chu SS, Jiang GH. Feeding deterrents from *Zanthoxylum schinifolium* against two stored-product insects. J Agric Food Chem. 2009;57(21):10130–3.
30. Zou H, Guo G, Wang M, Cao J, Huang G. Isolation of quinolone alkaloids from *Tetradium ruticarpum* via preparative high-speed counter-current chromatography and evaluation of their binding affinities for bovine serum albumin. Acta Chromatogr. 2018;30(2):73–80.
31. Tang YQ, Feng XZ, Huang L. Quinolone alkaloids from *Evodia rutaecarpa*. Phytochemistry. 1996;43(3):719–22.
32. Wang XX, Zan K, Shi SP, Zeng KW, Jiang Y, Guan Y, et al. Quinolone alkaloids with antibacterial and cytotoxic activities from the fruits of *Evodia rutaecarpa*. Fitoterapia. 2013;89:1–7.
33. Jin HZ, Du JL, Zhang WD, Chen HS, Lee JH, Lee JJ. A novel alkaloid from the fruits of *Evodia officinalis*. J Asian Nat Prod Res. 2007;9(7):685–8.
34. Jin HZ, Du JL, Zhang WD, Yan SK, Chen HS, Lee JH, et al. A new quinazolinedione alkaloid from the fruits of *Evodia officinalis*. Fitoterapia. 2008;79(4):317–8.
35. Heredia Y, Escalona Arranz J, Gonzalez Fernandez R, Ochoa Pacheco A, García Díaz J, Monzote L, et al. Trypanocidal potentialities of skimmianine an alkaloid isolated from *Zanthoxylum pistaciifolium* Griseb leaves. Pharmacogn Res. 2020;12(3):322–7.
36. Bi R, Yang XN, Zhou HF, Peng LY, Liu JX, Zhao QS. Eleven undescribed alkaloids from the rhizomes of *Sinomenium acutum* and their IDO1 and TDO inhibitory activities. Phytochemistry. 2022;200:113244.
37. Su XL, Xu S, Shan Y, Yin M, Chen Y, Feng X, et al. Three new quinazolines from *Evodia rutaecarpa* and their biological activity. Fitoterapia. 2018;127:186–92.
38. Pan TM, Ye JH, Li JN, Gui K, Li J, Feng JT, et al. Discovery of terpene-derived quaternary ring compounds containing an oxime moiety as potential fungicides. J Agric Food Chem. 2023;71(7):3164–72.
39. Yang ZH, Sun XB, Jin DJ, Qiu YG, Chen LL, Sun L, et al. Novel camphor sulfonohydrazide and sulfonamide derivatives as potential succinate dehydrogenase inhibitors against phytopathogenic fungi/oomycetes. J Agric Food Chem. 2023;71(1):174–85.
40. An JX, Wang R, Li AP, Zhang W, Nan ZB, Jiang WQ, et al. Prenylated flavonoids isolated from the root of *Sophora flavescens* as potent antifungal agents against *Botrytis cinerea*. J Agric Food Chem. 2024;72(36):19618–28.

Publisher's Note